CRYSTAL GROWTH & DESIGN

Article

pubs.acs.org/crystal

Detergent-Mediated Formation of β-Hematin: Heme Crystallization Promoted by Detergents Implicates Nanostructure Formation for Use as a Biological Mimic

Rebecca D. Sandlin,[‡,⊥] Kim Y. Fong,[‡,⊥] Renata Stiebler,[‡,#] Christopher P. Gulka,[‡] Jenny E. Nesbitt,[‡] Matheus P. Oliveira,[§] Marcus F. Oliveira,[§] and David W. Wright*[,‡]

[‡]Department of Chemistry, Vanderbilt University, Nashville, Tennessee, United States

[#]Laboratório de Biologia Celular, Instituto Oswaldo Cruz, Fundação Oswaldo Cruz, Rio de Janeiro, Brazil

[§]Laboratório de Bioquímica de Resposta ao Estresse, Programa de Biologia Molecular e Biotecnologia, Instituto de Bioquímica Médica, Leopoldo de Meis, Universidade Federal do Rio de Janeiro, Rio de Janeiro, RJ, Brazil

Supporting Information

ABSTRACT: Hemozoin is a unique biomineral that results from the sequestration of toxic free heme liberated as a consequence of hemoglobin degradation in the malaria parasite. Synthetic neutral lipid droplets (SNLDs) and phospholipids were previously shown to support the rapid formation of β-hematin, abiological hemozoin, under physiologically relevant pH and temperature, though the mechanism by which heme crystallization occurs remains unclear. Detergents are particularly interesting as a template because they are amphiphilic molecules that spontaneously organize into nanostructures and have been previously shown to mediate β-hematin formation. Here, 11 detergents were investigated to elucidate the physicochemical properties that best recapitulate crystal formation in the parasite. A strong correlation between the detergent's molecular structure and the corresponding kinetics of β-hematin formation was observed, where higher molecular weight polar chains promoted faster reactions. The larger hydrophilic chains correlated to the detergent's ability to rapidly sequester heme into the lipophilic core, allowing for crystal nucleation to occur. The data presented here suggest that detergent nanostructures promote β-hematin formation in a similar manner to SNLDs and phospholipids. Through understanding mediator properties that promote optimal crystal formation, we are able to establish an in vitro assay to probe this drug target pathway.

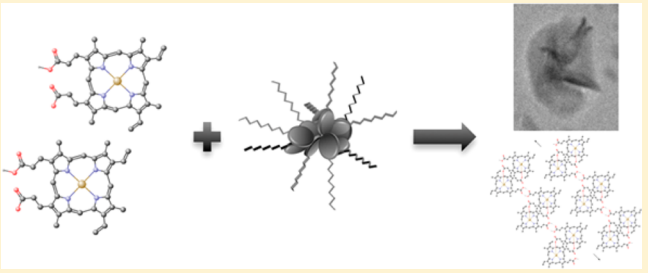

INTRODUCTION

Hemozoin is a unique biocrystalline material formed by several hematophagous organisms, from malaria parasites, to helminths, and even triatomine insects.[1−3] The hemozoin formation pathway is utilized in order to escape the effects of toxic free heme, which accumulates in these organisms as a consequence of hemoglobin catabolism. Though the discovery of hemozoin was reported as early as 1717,[4] the mechanism by which this crystal is produced is not yet fully understood and remains a subject of debate. The importance of understanding this crystallization pathway is underscored by the fact that hemozoin formation is an important drug target.[5] The quinoline antimalarials, such as chloroquine and quinine, act by building up noncrystallized heme levels, which ultimately results in parasite death.[6,7] Despite widespread resistance to quinoline compounds, hemozoin formation remains a suitable drug target pathway as the mechanism of resistance is completely separate from the drug mechanism of inhibition.[8] Synthetic strategies for hemozoin have been previously reported, though these approaches do not accurately reflect how heme molecules are crystallized within the parasite.[9−11] Biologically relevant *in vitro* models for hemozoin formation not only facilitate a better understanding of the *in vivo* formation of hemozoin, but are also useful in high-throughput screening (HTS) efforts for the development of new antimalarial drugs that target this parasite-specific pathway.[12]

Multiple research groups have conducted HTS in the search for novel antimalarial drugs, each with unique experimental parameters.[13,14] The efficiencies of the assays are most likely related to the variation in physicochemical conditions, ultimately causing drastic differences in hit rates. Our group previously established an HTS in vitro assay utilizing a lipophilic mediator mimic, Nonidet P-40 (NP-40), resulting in 171 antimalarial compounds out of the 530 β-hematin inhibitors tested (32%).[12] When compared to a previously reported assay, only 17 of the 644 (3%) β-hematin inhibitors identified in their HTS retained activity against *Plasmodium falciparum* cultures.[13] This difference in activity between

Received: November 6, 2015
Revised: March 7, 2016
Published: April 11, 2016

DOI: 10.1021/acs.cgd.5b01580
Cryst. Growth Des. 2016, 16, 2542−2551

screens is most likely due to assay conditions that better recapitulate parasite biology and the actual mechanism of hemozoin formation. With a drastic improvement in hit rate (>10-fold), it poses the question of why this particular detergent mediates crystal formation with such great success. Therefore, in an effort to better understand how detergents mediate in vitro heme crystallization, we studied their physicochemical properties.

Though the mechanism by which the parasite converts toxic free heme into nontoxic hemozoin is not completely agreed upon, one hypothesis has indicated a role for neutral lipid droplets (NLDs) in crystal formation. Micrographs have previously shown hemozoin crystals clearly associated with NLDs located in the acidic digestive food vacuole (pH 4.8).[15,16] Mass spectrometry analysis of the NLDs identified a blend of neutral lipids in a 4:2:1:1:1 ratio of monostearic, monopalmitic, dipalmitic, dioleic, and dilinoleic glycerols.[17] Recently, SNLDs composed of the same neutral lipid blend were shown to promote rapid formation of β-hematin ($t_{1/2}$ = 1.9 ± 0.01 min) under digestive vacuole conditions (pH 4.8, 37 °C).[18] Heme has also been shown to rapidly localize within these SNLDs in a pH-dependent manner that mirrors the pH dependence of β-hematin formation. Molecular dynamic simulations have further suggested that heme crystallization would be favored in a lipophilic environment providing more evidence that this process occurs at a lipid/water interface.[19]

An alternative model of hemozoin formation in *Plasmodium* spp. indicates through cryogenic synchrotron soft X-ray tomography that nucleation occurs at the inner surface of the digestive vacuole membrane instead of within NLDs.[20] Kapishnikov et al. showed hemozoin crystals to orient on the (100) and ($\bar{1}$00) faces, which allow for the polar head groups to be exposed and the free propionic acid groups of heme to hydrogen bond.[21] The crystals then grow along a curved surface parallel to each other along their needle *c* axes near the lipid/water interface.[22] This model also relies on heme interacting with lipids, allowing the current study to be of relevance in both hypotheses.

In addition to SNLDs, several synthetic routes for β-hematin formation have been reported including the use of alcohols, phospholipids, and lipophilic detergents.[11,23−26] Environmental conditions and the structure of these mediators affect β-hematin formation based on their amphipathic structures, charges, and polarity.[11,24,26] Huy et al. used alcohols to show that a lower surface tension of the aqueous interface reduces the energy barrier of crystal nucleation, increasing the rate of β-hematin formation.[11] The Oliveira group has studied the role of phospholipids in heme crystallization and demonstrated that β-hematin can be rapidly and efficiently produced by glycerophospholipids, especially unsaturated phosphatidylethanolamine and phosphatidylcholine, giving rise to very regularly shaped crystals similar to those produced in vivo.[25] Huy illustrated a similar effect of phospholipid melting temperature on the conversion of β-hematin and found results analogous to those of Stiebler et al.[25,26]

Detergents are amphiphilic molecules and are particularly interesting as a crystallization template due to their behavior in an aqueous environment. Detergents can exist in a variety of structures ranging from monomers to larger aggregate structures. Formation of these nanostructures is highly dependent on the chosen experimental conditions including pH, temperature, concentration, and the presence of ions. Interestingly, these nanostructures are similar in morphology to the SNLDs and may provide a suitable environment for β-hematin formation. Several detergents have previously been shown to promote heme crystallization, though the phase structure of the detergent was not determined.[23] Since no detailed, systematic investigation into detergent-mediated β-hematin formation has previously been reported, many questions regarding this process remain. Here, we investigated 11 detergents as mediators for β-hematin formation using physiologically relevant conditions of the digestive food vacuole (pH 4.8, 37 °C). The rate of β-hematin formation was established for each of the detergent mediators, and the phase structure that promotes β-hematin formation was determined using melting temperatures, critical micelle concentrations (CMC), and particle sizes. In addition, these studies help establish detergent properties that best resemble hemozoin formation *in vivo* for subsequent use in β-hematin formation in vitro assays.

EXPERIMENTAL SECTION

Materials. All Triton X detergents (45, 114, 100, 102, 165, and 305) were purchased from Sigma-Aldrich. Flat bottom, 384-well plates (3680, Corning) and 3-[(3-cholamidopropyl) dimethylammonio]-1-propanesulfonate (Pierce) were purchased from Fisher Scientific. Hemin (≥98%, Fluka), amodiaquine, sodium acetate trihydrate, Tween-20, Tween-80, sodium dodecyl sulfate, and pyridine were obtained from Sigma-Aldrich. Nonidet P-40 (Shell Chemical Co.) was purchased from Pierce Biotechnology, Rockford, IL, and is not to be confused with detergents from other companies also referred to as NP-40.

Determination of Optimal Detergent Concentration. The optimal detergent concentration (defined as the concentration that promotes maximum β-hematin formation) was determined for each of the 11 detergents using a multiple comparison one-way ANOVA to evaluate significance. The range of detergent concentration varied from 1 to 400 μM. Each detergent was solubilized in water (800 μM) and added in the appropriate volume to a 384-well flat bottom clear microtiter plate. The total volume in each well was then adjusted to 25 μL using water, followed by a 7-μL addition of acetone. A 25 mM stock solution of hematin was prepared by dissolving hemin chloride in DMSO followed by 1 min of sonication. The hematin solution was then filtered through a 0.22 μM PVDF membrane filter unit, was added to a 2 M acetate buffer (pH 4.8), and was vortexed to make the "heme stock" suspension (100 μM). We refer to the hematin species as heme throughout the manuscript. Twenty-five microliters of this heme stock was rapidly added to the microtiter plate followed by incubation in a 37 °C shaking water bath for 24 h. Free heme was then quantified using the pyridine-ferrochrome method[27] by adding 15 μL of acetone to each well of the plate, followed by 8 μL of pyridine solution (50% pyridine, 20% acetone, and 200 mM HEPES, pH 7.4) so that the final concentration of pyridine was 5% (v/v). After a 30 min shaking interval, the absorbance was measured at 405 nm on a BioTek H4 plate reader.[12]

Kinetic Investigations of Detergent Mediated β-Hematin Formation. The half-life of β-hematin formation was determined for each detergent at a concentration of 50 μM (the lowest concentration at which β-hematin formation is observed for all detergents). Stock solutions of each detergent were prepared in 2 M acetate buffer (pH 4.8). To 1.5 mL microcentrifuge tubes, 400 μL of the detergent stock was added. The tubes were preincubated in a 37 °C water bath for 15 min, followed by the addition of 400 μL of a 100 μM heme stock suspension in prewarmed acetate buffer. The tubes were shaken at 45 rpm, and triplicate sample tubes were removed from the water bath at regular intervals. β-Hematin formation was analyzed using the pyridine-ferrochrome method of quantification described above with half-lives ($t_{1/2}$) and standard deviations were generated using GraphPad Prism v5.0.

Characterization of β-Hematin Product. Following formation of β-hematin with each detergent mediator at the optimal detergent

DOI: 10.1021/acs.cgd.5b01580
Cryst. Growth Des. 2016, 16, 2542−2551

concentration as previously described, the product was washed thoroughly with a pyridine solution (5% pyridine, 20% acetone, water, and 200 mM HEPES, pH 7.4) three times to remove excess free heme. The crystal product was washed again three times with water and dried. X-ray diffraction (XRD) was utilized to confirm the identity of each dried, homogenized product. Measurements were collected using Cu Kα radiation (λ = 1.541 Å), with data collection on a Scintag Int. (U.S.A.) instrument with a vertical goniometer in the 2θ range of 5−40°. β-Hematin was suspended in acetone, and the external morphology of the crystals was examined using a Philips CM20 transmission electron microscope (TEM) on Formvar coated Cu grids.

Detergent Phase Transition Melting Temperatures. Phase transition temperatures of the detergents were determined by differential scanning calorimetry (DSC) on a TA Instruments DSC Q1000. The samples consisted of pure detergents as obtained from the supplier pressed in aluminum standard pans. Each sample was equilibrated at 100 °C for 5 min followed by three cycles of scans ranging from 100 °C to −100 °C at 10 °C/min and back up to 100 °C with 5 min isothermal steps at each end of the cycle. Melting transitions were determined from heat−cool−heat plots showing changes in heat flow with respect to time and temperature and analyzed using Universal V4.5A TA Instruments software.

Characterization of Detergent Nanostructure. The CMC of each detergent under assay conditions was determined using an Attension Sigma700 tensiometer. The concentrations tested ranged from 5 μM to 1 mM for all detergents, except for 3-[(3-cholamidopropyl)dimethylammonio]-1-propanesulfonate (CHAPS), which spanned a broader range of 5 μM to 11 mM. Stock solutions (2 mM) of each detergent were prepared in a 1 M acetate buffer (pH 4.8), and the appropriate volume of stock was added to a 50 mL conical tube and diluted to the desired concentration with additional acetate buffer. The higher concentration solutions for CHAPS were prepared by weighing out the appropriate mass into 50 mL conical tubes and diluting with acetate buffer. The tubes were preincubated in a 37 °C water bath for 1 h. Sample tubes were removed from the bath and placed in a temperature-controlled environment while the surface tension was measured using a Du Noüy ring. CMCs were generated using segmented linear regression fitting methods with GraphPad Prism v5.0, as described by Provera et al.[28]

Dynamic light scattering (DLS) was utilized to investigate the size distribution of the detergents under experiment conditions. Each detergent was prepared in 1 M acetate buffer at the optimal concentration of detergent (described above). The detergents were then equilibrated for 15 min at 37 °C. A pipet was then used to carefully transfer the solution to a cuvette and analyzed using a Malvern Zetasizer with a lower limit of 0.1 nm and an upper limit of 6 μm. Triplicate samples were prepared and analyzed with standard deviation reported.

Heme Solubilization and Crystallization. The effect of detergents on heme solubility was determined using a method previously described by Stiebler et al.[24] Briefly, hemin in 1% DMSO (100 μM final concentration) was mixed with each detergent (10 mM) in 1 M sodium acetate buffer (pH 4.8) for 10 min. Following centrifugation at 17100g for 5 min, the supernatants were collected. To quantify the amount of free heme remaining in solution, a 300-μL aliquot was added to 700 μL of an alkaline-pyridine solution (48% pyridine, 200 mM NaOH) and measured absorbance on a Synergy H4 Hybrid Plate Reader (BioTek) between 300−700 nm.

Heme crystallization was calculated for each detergent following formation of β-hematin product, as previously described in the section above titled Kinetic Investigations of Detergent Mediated β-Hematin Formation. An incubation time of 120 min was chosen since it was the average half-life for all detergents. Free heme was quantified using the pyridine-ferrochrome method with the mass-balance of heme starting material converted into β-hematin crystals.[14]

Data Analysis Using the Avrami Equation. The kinetics of β-hematin formation were analyzed using linear least-squares fitting methods with GraphPad Prism v5.0 and then fitted to the Avrami equation:

$$Y = c(1 - e^{-zt^n}) \quad (1)$$

where Y is the mass percentage of β-hematin formed, c is the maximum percentage of β-hematin formed at the end of the reaction, z is an empirical rate constant, t is time, and n is the Avrami constant. Kinetics data were fit to n = 1, 2, 3, and 4. The curve that represented the best fit based on the r^2 value was reported as the appropriate Avrami constant that represents the crystallization process.

RESULTS AND DISCUSSION

Eleven detergents were selected to study the role of detergents as lipophilic mediators to then apply these results in the optimization of an in vitro β-hematin formation assay. These detergents include Tween 20, Tween 80, sodium dodecyl sulfate (SDS), CHAPS, NP-40, and six detergents from the Triton X series (Figure 1). Ionic SDS and the zwitterionic

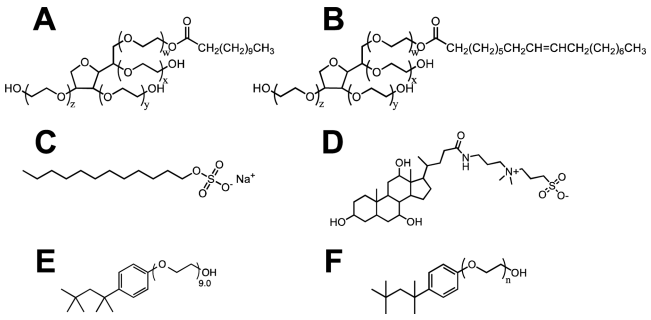

Figure 1. Eleven detergents used in this investigation include (A) Tween 20, where $w + x + y + z$ = 20, (B) Tween 80, where $w + x + y + z$ = 20, (C) SDS, (D) CHAPS, (E) NP-40, and (F) the TX_n detergents where n = 4.5, 7.5, 9.5, 12, 16, or 30.

detergent CHAPS were obtained to examine the effects of charged functional groups on β-hematin formation. Tween 20 and Tween 80 are both nonionic detergents with identical poly(ethylene oxide) (PEO) hydrophilic head groups, and Tween 20 has previously been shown to facilitate β-hematin formation.[29] These two detergents can be distinguished by the length of their fatty acid ester moiety: the 11 carbon hydrophobic tail of Tween 20 is saturated, while the 17 carbon tail of Tween 80 contains a double bond. NP-40 and the Triton X series of detergents were selected due to the PEO hydrophilic portion of the detergent, which is similar to the glycerol hydrophilic portion of neutral lipids. Further, the Triton X detergents allow a systematic examination of the effects of PEO chain length on β-hematin formation. The six Triton X detergents obtained are Triton X-45, -114, -100, -102, -165, and -305 with average side chains of 4.5, 7.5, 9.5, 12, 16, and 30 PEO units, respectively. NP-40 has an average PEO chain length of 9.0. For simplicity, the Triton X detergents will be referenced as TX_n where n specifies the average size of the PEO side chain length.

Detergents Promote β-Hematin Formation. β-Hematin formation was measured using a range of concentrations (1−400 μM) for each of the detergents in this study. The Tween, NP-40, and TX_n detergents each yielded 76−88% β-hematin product, whereas SDS and CHAPS only yielded 40 and 51% product, respectively (Table 1). The yields obtained here are similar to those found for comparable amphiphilic phospholipids such as phosphatidylcholine, phosphatidylethanolamine, and phosphatidylserine in a previous study.[25] The minimum concentration at which maximum β-hematin formation was observed is referred to herein as the optimal detergent

DOI: 10.1021/acs.cgd.5b01580
Cryst. Growth Des. 2016, 16, 2542−2551

Table 1. Optimal Detergent Concentration, the Minimum Concentration That Promotes Maximal β-Hematin Formation, Was Determined for Each of the Detergents along with the Yield of β-Hematin Formation Using a Multiple Comparison One-Way ANOVA to Evaluate Significance[a]

detergent name	abbreviation	optimal concentration (μM)	% β-hematin formation
lipid blend	SNLDs	50	89
Tween 20		10	87
Tween 80		15	82
sodium dodecyl sulfate	SDS	1140	40
(3-((3-cholamidopropyl) dimethylammonio)-1-propanesulfonate)	CHAPS	1465	51
Nonidet P-40	NP-40	30	88
Triton X-45	$TX_{4.5}$	50	86
Triton X-114	$TX_{7.5}$	40	80
Triton X-100	$TX_{9.5}$	30	80
Triton X-102	TX_{12}	20	80
Triton X-165	TX_{16}	10	76
Triton X-305	TX_{30}	5	79

[a]The detergents were solubilized in water and incubated at 37 °C while shaking for 24 h.

each of the 11 detergents at 50 μM, pH 4.8, 37 °C (Table 2). Tween 20, Tween 80, and SDS facilitated rapid formation of β-hematin with $t_{1/2}$ of 5.9 ± 0.2, 7.4 ± 0.2, and 3.7 ± 0.2 min, respectively. The $t_{1/2}$ of CHAPS was significantly higher at 628.5 ± 31.0 min (Figure SI1). The β-hematin product initiated by Tween 20, Tween 80, and SDS exhibited instantaneous growth profiles, whereas sigmoidal growth was observed in the case of CHAPS. This significant increase in the $t_{1/2}$ of β-hematin formation suggests that CHAPS-mediated β-hematin formation is not comparable to that observed for SNLDs or phospholipids.[25]

Table 2. Detergent-Mediated $t_{1/2}$ of β-Hematin Formation Calculated through the Pyridine-Ferrochrome Method Following Incubation of a 50 μM Heme Solution with Each Detergent at 50 μM, the Lowest Concentration That β-Hematin Was Observed for the Triton X Series[a]

detergent name	$t_{1/2}$ (min)
Tween 20	5.9 ± 0.2
Tween 80	7.4 ± 0.2
SDS	3.7 ± 0.2
CHAPS	628.5 ± 31.0
Nonidet P-40	52.9 ± 2.1
Triton X-45	546.4 ± 23.4
Triton X-114	227.8 ± 5.6
Triton X-100	165.0 ± 2.9
Triton X-102	139.9 ± 1.4
Triton X-165	110.5 ± 1.7
Triton X-305	93.4 ± 0.8

[a]Samples were incubated at 37°C and pH 4.8 while shaking with triplicate aliquots removed at regular time intervals. The average half-life with standard deviation was calculated using the sigmoidal dose-response (variable slope) analysis on GraphPad Prism v5.0.

concentration (Figure 2A). For Tween, NP-40, and TX_n detergents, the optimal detergent concentration was within the range of 5−50 μM (Table 1), comparable to the SNLDs. A closer examination of NP-40 and the TX_n mediators reveals the optimal detergent concentration decreases as a function of increasing values of n (Figure 2B). Specifically, as the PEO chain length increases, lower concentrations of detergent are required to reach the saturation point of β-hematin formation. SDS and CHAPS-mediated β-hematin formation was achieved only at higher concentrations of detergent, requiring ∼1.1 mM and 1.5 mM detergent concentration, respectively. Also, the products obtained from SDS and CHAPS were less stable than that obtained from other detergents since loss of product was observed upon washing with 5% pyridine, suggesting heavy contamination with non-β-hematin products such as heme dimers, partially hydrated heme, or oligomeric heme aggregates.

Kinetics of Detergent-Mediated β-Hematin Formation. The kinetics of β-hematin formation was determined for

Characterization of β-Hematin Product. Heme was incubated with each of the detergents for 24 h at the optimal concentration under digestive vacuole environmental conditions (37 °C and pH 4.8). Morphological and structural analyses of the products obtained confirmed the presence of β-hematin for all detergents. XRD patterns of products were consistent with that of hemozoin and β-hematin (Figures 3 and SI2).[30,31] The reported XRD pattern was reproduced using the atomic coordinates listed for β-hematin, which include the

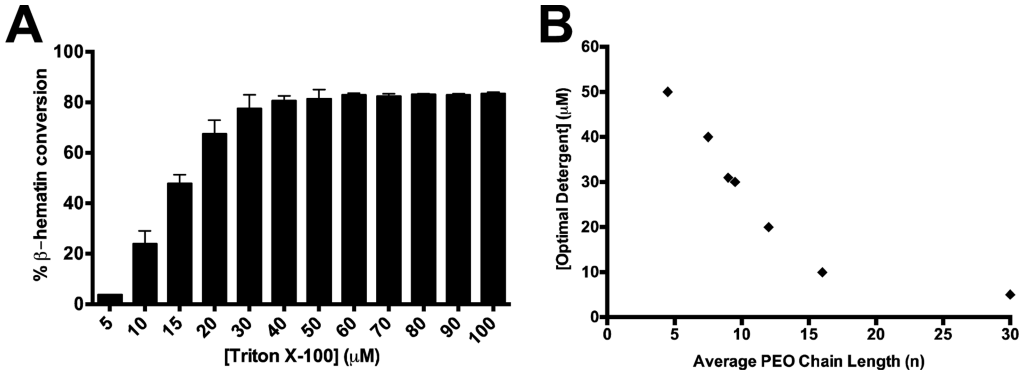

Figure 2. (A) The mean percent and standard deviation of β-hematin formed was measured using a range of detergent concentrations. The optimal detergent concentration of Triton X-100 detergent was found to be 30 μM, the lowest concentration at which maximum β-hematin was observed, determined by a multiple comparison one-way ANOVA test. (B) The optimal detergent concentration of NP-40 and the Triton X detergents varies with respect to the PEO side chain length (n).

DOI: 10.1021/acs.cgd.5b01580
Cryst. Growth Des. 2016, 16, 2542−2551

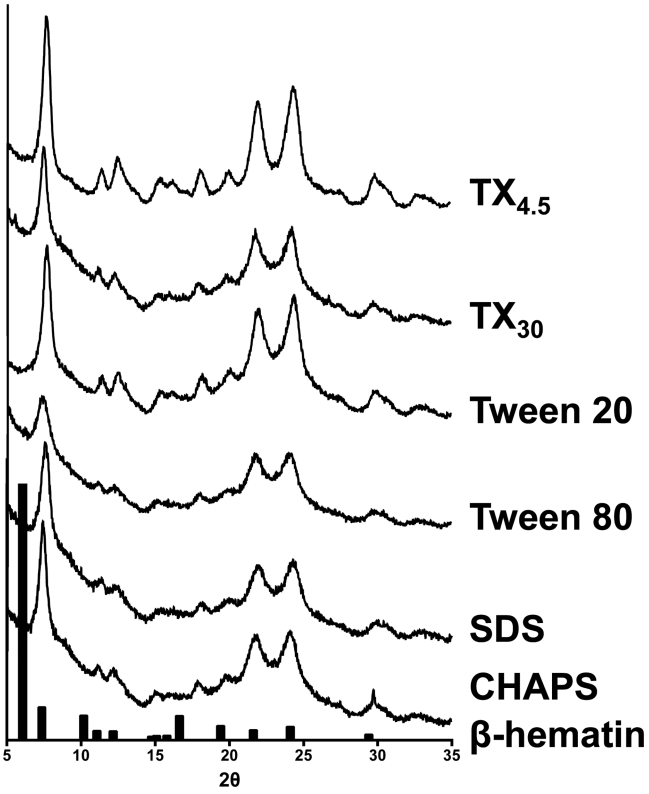

Figure 3. XRD patterns of the β-hematin products obtained through incubation of heme with the detergent mediators. The XRD pattern of β-hematin synthesized by the aqueous acid-catalyzed method by Slater et al. is shown in the black bars.[33]

characteristic diffraction peaks at 7.4°, 21.7°, and 24.3° and was used to compare the crystals formed by the detergents in this study.[30,32] The external morphology of the products observed through TEM exhibits well-formed crystals resembling hemozoin for Tween, NP-40, TX_n, and CHAPS detergents (Figure 4 and SI3). These crystals range from 200−1000 nm in size, similar to β-hematin formed by NLDs and phospholipids.[25,34,44] For SDS, fewer well-formed β-hematin crystals are present and more irregularity is apparent (Figure 4E). The morphological differences and inefficiency of CHAPS and SDS mediated β-hematin formation may be a result of their phase transition melting points (T_m = 157 and 206 °C, respectively).[35] These melting temperatures are significantly above experimental conditions, causing the detergent structures to have increased rigidity. The lack of fluidity may hinder β-hematin formation due to decreased heme accessibility into the lipophilic core. NP-40 and the TX_n series were found to have phase transition temperatures around or below the experimental temperature (37 °C), allowing some fluidity in the detergent aggregates and β-hematin to form (Figure 5). The deviation of CHAPS- and SDS-mediated β-hematin from the behavior observed by SNLDs may be from the strong interactions between their polar head groups and suggests that these two detergents do not serve as model systems for SNLDs.

Characterization of Detergent Structures and the Effect on β-Hematin Formation. To initiate growth of the β-hematin crystal, the porphyrin rings of two heme molecules overlap through $\pi-\pi$ interactions forming columnar aggregates of dimeric units. Extension in a second dimension results from metal-propionate linkages between dimers, which help stabilize

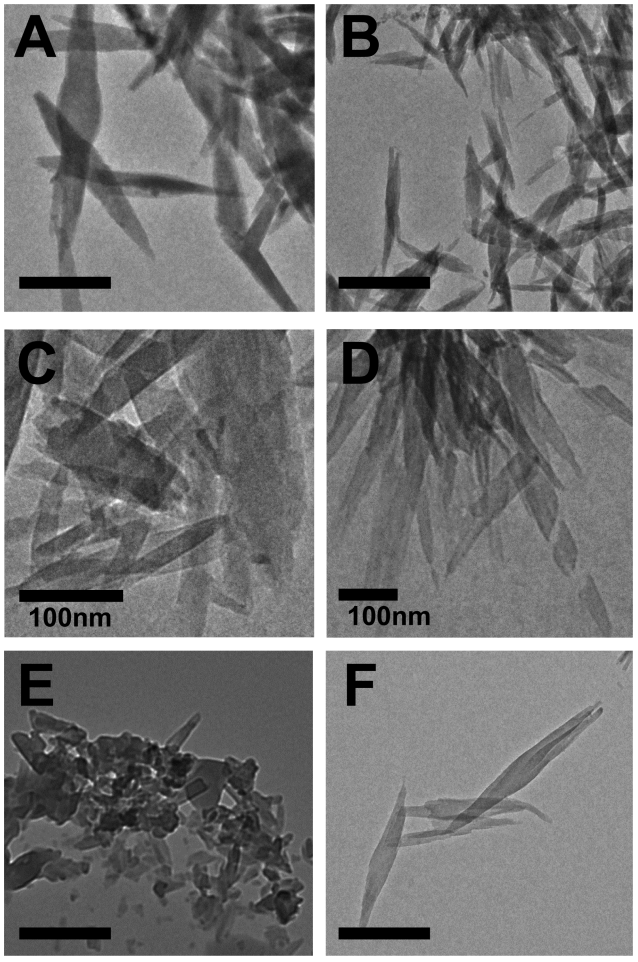

Figure 4. External morphology of product obtained from incubation of heme with (A) $TX_{4.5}$, (B) TX_{30}, (C) Tween 20, (D) Tween 80, (E) SDS, and (F) CHAPS at pH 4.8 and 37 °C reveal well-formed crystals that resemble hemozoin. In the case of SDS, fewer well-formed crystals are present. Scale bars are 500 nm unless otherwise indicated.

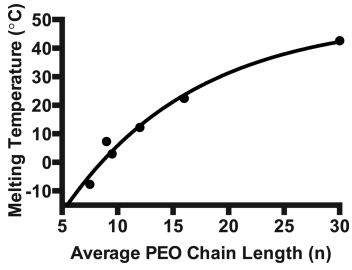

Figure 5. Phase transition melting temperatures determined by differential scanning calorimetry. Melting transition temperatures were determined following three cycles of heat−cool−heat scans. Longer hydrophilic chains (n) correlate to a higher melting temperature among NP-40 and the Triton X series of detergents.

the crystal structure in the aqueous digestive vacuole.[36] Formation of this linkage requires the displacement of axial water molecules from the Fe(III) center of heme. Using molecular dynamic simulations, Egan and co-workers demonstrated that displacement of the water molecule is favored under lipophilic conditions, such as the environment offered by NLDs, phospholipids, or detergents. Previous studies have demonstrated that several detergents promote formation of β-hematin, though the role of detergent dynamics in this process

DOI: 10.1021/acs.cgd.5b01580
Cryst. Growth Des. 2016, 16, 2542−2551

was not studied.[23] Because of the similarity between NLDs and detergent nanostructures, we suspected that the optimal detergent concentration required for β-hematin formation correlated with the presence of a similar environment of structured amphiphilicity and was also affected by detergent CMCs.

While a relationship between hydrophilic chain length and detergent CMC was observed (Figure 6A), NP-40 and the TX_n

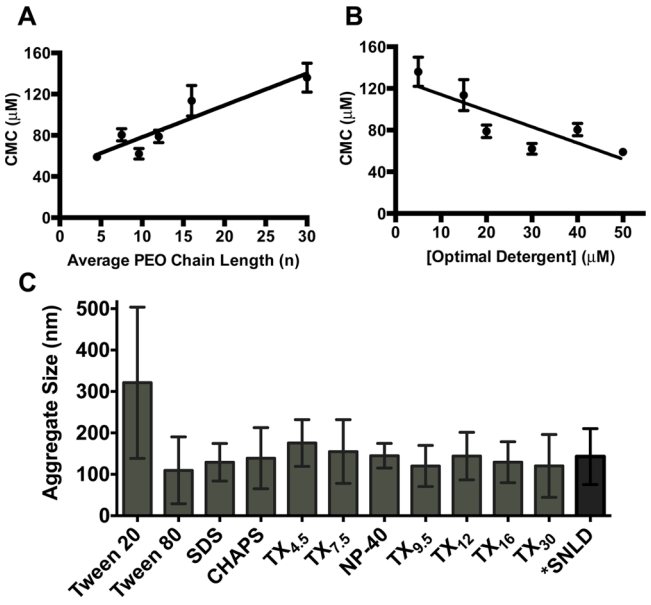

Figure 6. (A) A positive relationship is observed between the CMC (mean and standard deviation of three replicates) for the Triton X series of detergents and the average length of the hydrophilic PEO side chain. (B) The optimal detergent concentration for each detergent is less than the CMC (mean and standard deviation) under assay conditions, indicating structured micelles are not required for β-hematin formation. (C) Average size of detergent aggregates measured at the optimal detergent concentration under assay conditions with standard deviations reported (pH 4.8, 37 °C) using DLS. *Data from Ambele et al.[34]

detergent structures did not abide by the definition of a micelle at their optimal concentrations since these values were lower than their CMCs determined under assay conditions (37 °C and pH 4.8) (Figure 6B). The detergents form aggregates instead of micelles since at the optimal detergent concentration a single, albeit broad, peak was observed by DLS under identical conditions (Figure 6C). Nonetheless, this supports the hypothesis that a hydrophobic environment is required in order for the water ligand to be released from the iron center and the coordination of a propionate group of a second heme molecule to occur. The amphiphilic aggregate structure still allows for the sequestering and solubilizing heme to form β-hematin crystals. According to DLS measurements, the size distribution of the detergents ranged from ~100−300 nm, in agreement with TEM images obtained (Figures 6C and SI4). Since micelles are typically <20 nm in diameter, these results support that under assay conditions the detergents likely form aggregates, still possessing structure based on polarities. This size distribution is consistent with that previously reported for SNLDs.[18]

Detergent Effects on Heme Solubilization and Crystallization. Concentrated within the digestive food vacuole, NLDs are thought to serve as a reservoir for amphiphilic heme upon release from hemoglobin.[18,37] In support of this hypothesis, recent reports have revealed that it is unlikely for β-hematin to form in an aqueous medium, implying that a lipid environment would aid in the initial solubilization of heme,[38,44] similar to the ideal environment reported with phospholipid mediated β-hematin formation.[24] In this lipophilic environment, displacement of the axially coordinated water would be favored, a step which must precede formation of the propionate-iron linkage that comprises the heme dimer. The effect of hydrophobicity on heme solubilization was assessed through comparing NP-40 and the TX_n series of detergents. A 10 mM detergent solution in acetate buffer (pH 4.8) was incubated with 100 μM heme in DMSO for 10 min followed by quantification of solubilized heme by the alkaline-pyridine method.[39] We found that the aggregates solubilize heme and follow the trend of TX_{30}> TX_{16} > TX_{12} > $TX_{9.5}$ > NP-40 > $TX_{7.5}$ > $TX_{4.5}$, facilitating heme to be sequestered into the hydrophobic core, and resulting in the increased solubility of heme early on in crystallization (Figure 7A). This is consistent with previous trends found with these PEO containing detergents as well as with organic solvents, which result in faster β-hematin formation and lower optimal detergent concentrations with longer chain lengths.[24]

The current explanation for β-hematin formation in SNLDs or phospholipids can be used to rationalize detergent-mediated heme solubilization and its further crystallization. In SNLDs, amphiphilic heme has been shown to rapidly partition within the hydrophobic interior of the lipid particle.[18] The TX_n detergents differ only in the hydrophilic portion of the molecule, which implies the correlation between increased heme crystallization and β-hematin formation as a function of PEO chain length is dependent upon interactions that occur with heme and the hydrophilic surfaces. Therefore, this trend could arise from the rate at which heme is sequestered into the hydrophobic portion of the detergent aggregate where β-hematin formation is proposed to occur. For the TX_n detergents, a greater number of PEO units corresponds to a smaller aggregation number; therefore, we would expect the surfaces of the TX_n detergents to be relatively equally packed and form similar sized aggregates.[40] However, a longer hydrophilic chain would still allow for a greater probability for the heme to interact with the PEO units and to be sequestered into the hydrophobic core at a more rapid rate compared to detergents with shorter hydrophilic chains. This situation is analogous to SNLDs and phospholipids where lower activation barriers for heme crystallization are observed for lipids with less rigid surfaces.[25,26,40] The increased fluidity of TX_n detergents with smaller PEO chains, as indicated by their phase transition temperatures, allows for faster organization of heme molecules, resulting in dimer assembly and crystal nucleation.

To facilitate a systematic investigation into the effects of structural variations of the detergents on β-hematin formation, the kinetics of NP-40 and the TX_n detergents were analyzed again, but instead at a consistent concentration among all samples (50 μM), where saturation of product has been reached for all detergents. This is the minimal concentration at which these detergents were observed to form product over 24 h. For each detergent, β-hematin formation followed a sigmoidal growth profile with average half-lives ranging from 93.4−546.4 min (Figure 7B). This type of growth is consistent with a crystallization processes consisting of a nucleation and growth phase reflecting an initial induction phase followed by rapid product formation based on the Avrami best-fit equation

DOI: 10.1021/acs.cgd.5b01580
Cryst. Growth Des. 2016, 16, 2542−2551

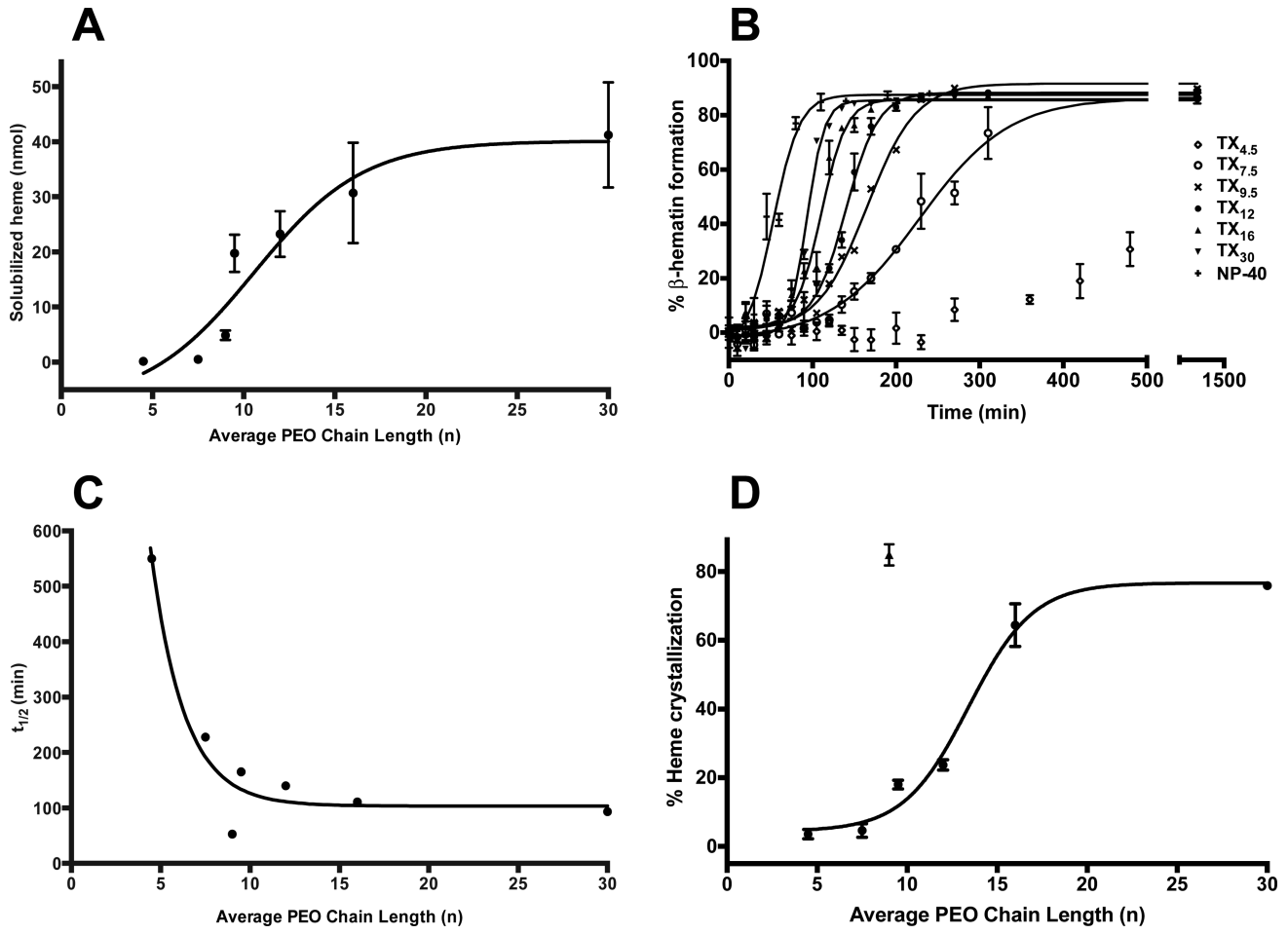

Figure 7. (A) The amount of solubilized heme was quantified after 10 min for NP-40 and the TX_n detergents using the pyridine-ferrochrome method. The amount of solubilized heme increased in a sigmoidal pattern with increasing PEO lengths. Measurements were taken in triplicate with reported standard deviations. (B) TX_n-mediated β-hematin formation follows a sigmoidal growth pattern. The value of n is indicated for each of the kinetic growth curves. (C) The $t_{1/2}$ of β-hematin formation was determined for each of the TX_n detergents, with a shorter chain length resulting in a longer half-life. (D) The percentage of heme crystallization was determined after 120 min of incubation with the TX_n detergents (circles) revealing a similar pattern to the amount of heme solubilized by the detergent mediators. NP-40 (triangle) resulted in much faster kinetics with a greater amount of crystallized heme formed at 120 min compared to all other detergents. Measurements were taken in triplicate with reported standard deviations.

(discussed further in the following section). This analysis reveals that the $t_{1/2}$ of β-hematin formation correlates to the length of the PEO side chain where the half-life of $TX_{4.5}$ > $TX_{7.5}$ > $TX_{9.5}$ > TX_{12} > TX_{16} > TX_{30} (Figure 7C). NP-40 resulted in the shortest $t_{1/2}$ (52.9 ± 2.1 min), which is more representative of the physiological rate of β-hematin formation. We suspected this trend could result from the increased β-hematin crystallization in acidic medium. To investigate this trend further, the amount of β-hematin crystallization was determined for each detergent following 120 min of incubation at 37 °C. Figure 7D reveals a sigmoidal curve between the percentage of crystallized β-hematin and the average PEO chain length for the detergents, similar to the trend seen with solubilized heme. This observation provides support for the hypothesis that as the PEO length increases, more rapid β-hematin formation occurs due to increased initial heme solubilization, which favors heme crystallization.

Since aggregate sizes are relatively uniform among each detergent (Figure 6C), the differences in heme solubilization and crystallization are most likely not due to detergent particle size, but from other detergent properties. Phase transition temperature (T_m) is one of the main physicochemical factors responsible for heme crystallization activity mediated by phospholipids and is affected by the size and unsaturation of the acyl chains, as well as the polar head groups (Figure 5).[25,26] Similarly in the present study, detergent polarity and PEO chain length affects the kinetic efficiency of mediated β-hematin formation (Figure 7C).

Nucleation and Growth of β-Hematin Crystals. The sigmoidal growth profile observed for detergent-mediated β-hematin formation is typical of a crystallization process and is reflective of a nucleation and growth phase where an initial induction phase of ~20 min is observed, followed by rapid product formation. The Avrami equation is frequently used to model this nucleation and growth process (see Experimental Section).[41] In this equation, the Avrami constant, n, represents the type of nucleation and dimensionality of crystal growth and typically takes an integer value where n = 1, 2, 3, or 4. The kinetics data at a 50-μM concentration were fit to the Avrami equation and constrained to each of the four integer values of n (Figure SI5). Table 3 lists the best-fit value of n obtained from each of the detergent mediators. NP-40 and all TX_n detergents

DOI: 10.1021/acs.cgd.5b01580
Cryst. Growth Des. 2016, 16, 2542−2551

Table 3. Best-Fit Value of the Avrami Equation Was Determined for Each of the Detergents[a]

detergent name	n	r^2	z (min^{-n})[b]
Tween 20	1	0.94	0.12 ± 0.02
Tween 80	1	0.96	0.11 ± 0.01
NP-40[c]	4	0.97	$7.26 \pm 1.40 \times 10^{-8}$
Triton X-45	4	0.99	$7.52 \pm 0.57 \times 10^{-12}$
Triton X-114[c]	4	0.97	$2.68 \pm 0.34 \times 10^{-10}$
Triton X-100	4	0.99	$9.65 \pm 0.77 \times 10^{-10}$
Triton X-102	4	0.99	$1.87 \pm 0.13 \times 10^{-9}$
Triton X-165	4	0.98	$4.92 \pm 0.52 \times 10^{-9}$
Triton X-305	4	0.99	$9.11 \pm 0.95 \times 10^{-9}$

[a]The kinetics of β-hematin formation were analyzed following incubation of a mixture of heme (50 μM) and detergent (50 μM) at 37 °C and pH 4.8 while shaking with the mean and standard deviations of three replicates reported. [b]The rate constant calculated based on the indicated Avrami constant, n. [c]Triton X-114 and NP-40 had a slightly better fit for n = 3.

conform to n = 3 or 4, in which n = 4 describes a system where nucleation is sporadic and spherical growth occurs in three dimensions. A constant of n = 3 can indicate either sporadic nucleation with growth in two dimensions or instantaneous nucleation with three-dimensional growth. Since structures formed by NP-40 and the TX_n detergent are similar in size (Figure 6C), and the resultant β-hematin product exhibits similar needle-like morphology (Figures 4 and SI3), it is likely that the crystallization process proceeds in a similar manner for each of the detergents. Indeed, each of these detergents except NP-40 and $TX_{7.5}$ exhibited best-fit values for the Avrami constant of n = 4, but since the fit to either integer value is nearly identical, we chose to use the value of n = 4 to describe the kinetics of these outliers (Table 3). This assignment is consistent with other crystallization systems that have been previously described.[24,42,43] Tween 20 and Tween 80 had excellent fits for n = 1 but deviated significantly for all other values of n. This fit indicates that crystal growth follows instantaneous nucleation and rod-like growth in one dimension. The instantaneous nucleation is reflected in the rapid formation of product for each of these detergents where the half-lives of Tween 20 and Tween 80 are 5.9 ± 0.2 and 7.4 ± 0.2 min, respectively. At 50 μM, CHAPS and SDS did not effectively form β-hematin to apply the Avrami equation, again indicating that these detergents are not appropriate substitutes when designing a biologically relevant in vitro assay.

Significant variations of the hydrophilic PEO portion of these molecules are made with no effect on the best-fit value for the Avrami constant. The variability of the Avrami constant between crystallization templates could therefore be due to the molecular interactions that occur between heme and the hydrophobic portion of the detergent. Specifically for the Tween detergents, the hydrophobic portion of the molecule is significantly larger than for the TX_n detergents. This could facilitate more rapid solubilization of free heme, resulting in instantaneous nucleation in the presence of the Tween vesicles leading to an Avrami constant of n = 1.

CONCLUSION

Detergents have been identified as mediators of β-hematin formation, though no systematic investigation into the effects of detergent identity on heme crystallization has previously been reported. Here we evaluated 11 detergents on their ability to form β-hematin under biologically relevant conditions in order to better understand the reason for enhanced hit rates in our HTS in vitro target-based assay compared to others. While β-hematin is not formed at a physiological relevant rate in buffer alone, the addition of a detergent mediator can decrease the rate of crystal formation to be comparable to that found within the parasite. We have found four physicochemical properties of the lipophilic mediator that affect β-hematin formation: charge of the polar headgroup, the hydrophobic core, hydrophilic chain length, and temperature.

The results reported here indicate detergent-mediated β-hematin formation occurs when there is a sufficient hydrophilic environment to allow for the organization of heme molecules. This can be seen in either aggregated forms or vesicles, with the longer hydrophilic portion facilitating a more rapid partitioning of the heme to the hydrophobic interior. These nanostructures would provide a hydrophilic−hydrophobic interface that would favor early heme partition and solubilization into the lipid layer. Heme molecules are thus able to orient in a suitable manner that reduces the energy barrier required to allow axial water removal and eventually allowing heme−heme interaction through reciprocal iron−carboxylate bonds. These nanostructures are able to closely mimic the hypotheses for hemozoin crystallization and growth along the lipid subphase found either as neutral lipid droplets in the DV or as phospholipids in the DV membrane.[22,44] Therefore, these detergents could be utilized as surrogates to study β-hematin formation in vitro and applied to assay development. Because of the wide availability and structural diversity of detergents, β-hematin formation was investigated in a systematic manner that has not been fully appreciated using lipid mediators. The advantage with detergents in understanding this drug target pathway is that the molecular organization of the mediating template can be easily manipulated by adjusting either the hydrophilic or hydrophobic portions of the detergent molecule. The resulting detergent nanostructures provide details on the physicochemical properties of the mediator that give rise to β-hematin formation leading to a more molecular-based understanding that can then be applied to in vitro assays. The results from this study help elucidate the molecular interactions of the lipophilic mediator with heme that facilitate the nucleation and formation of β-hematin. This information establishes properties of the lipid mediator required for crystal formation and subsequently establish a detergent most similar to the biological NLDs found within the malaria parasite.

ASSOCIATED CONTENT

Supporting Information

The Supporting Information is available free of charge on the ACS Publications website at DOI: 10.1021/acs.cgd.5b01580.

SI 1: Kinetic curves of detergent-mediated β-hematin formation. SI 2: XRD patterns of β-hematin products formed by various detergents. SI3: TEM images of β-hematin products formed by various detergents. SI4: TEM images of NP-40 and Triton X-305 detergent aggregates. SI5: Avrami kinetic curves of β-formation by Triton X-45 and Triton X-305 (PDF)

AUTHOR INFORMATION

Corresponding Author

*E-mail: david.wright@vanderbilt.edu.

DOI: 10.1021/acs.cgd.5b01580
Cryst. Growth Des. 2016, 16, 2542−2551

Author Contributions

[⊥]R.D.S and K.Y.F contributed equally.

Funding

This work was supported by grants from Conselho Nacional de Desenvolvimento Cientifico e Tecnológico (CNPq) (through Institutos Nacionais de Ciência e Tecnologia 2010), Fundação Carlos Chagas Filho de Amparo a Pesquisa do Estado do Rio de Janeiro (FAPERJ) (through Jovem Cientista do Nosso Estado E-26/101.492/2010; Cientista do Nosso Estado E-26/102.333/2013; Pronem E-26/111.169/2011). R.S. was a PAPD-FAPERJ fellow (Apoio à Pós-Doutorado no Estado do Rio de Janeiro, E-26/101.310/2014). M.P.O. was a CNPq undergraduate fellow (through Edital MCT/CNPq 110230/2008-6) and a graduate fellow (through Edital MCT/CNPq 151264/2010-4; 160357/2012-8). M.F.O. is a research scholar from CNPq (Produtividade em Pesquisa-PQ 301571/2009-0).

Notes

The authors declare no competing financial interest.

■ ACKNOWLEDGMENTS

The authors would like to thank M. F. Richards for critical reading of this manuscript. They would also like to thank Jeremiah C. Beam for assistance with X-ray diffraction experiments as well as Timothy C. Boire for the use of the differential scanning calorimeter.

■ ABBREVIATIONS

SNLD: synthetic neutral lipid droplet; HTS: high throughput screening; NP-40: Nonidet P-40; NLD: neutral lipid droplet; CMC: critical micelle concentration; XRD: X-ray diffraction; TEM: transmission electron microscopy; DSC: differential scanning calorimetry; CHAPS: 3-[(3-cholamidopropyl)-dimethylammonio]-1-propanesulfonate; DLS: dynamic light scattering; SDS: sodium dodecyl sulfate; PEO: poly(ethylene oxide); TX_n: Triton X detergents

■ REFERENCES

(1) Stiebler, R.; Correa Soares, J. B. R.; Timm, B. L.; Silva, J. R.; Mury, F. B.; Dansa-Petretski, M.; Oliveira, M. F. *J. Bioenerg. Biomembr.* **2011**, *43*, 93−99.
(2) Oliveira, M. F.; d'Avila, J. C.; Torres, C. R.; Oliveira, P. L.; Tempone, A. J.; Rumjanek, F. D.; Braga, C. M. S.; Silva, J. R.; Dansa-Petretski, M.; Oliveira, M. A.; de Souza, W.; Ferreira, S. T. *Mol. Biochem. Parasitol.* **2000**, *111*, 217−221.
(3) Oliveira, M. F.; Gandara, A. C. P.; Braga, C. M. S.; Silva, J. R.; Mury, F. B.; Dansa-Petretski, M.; Menezes, D.; Vannier-Santos, M. A.; Oliveira, P. L. *Comp. Biochem. Physiol., Part C: Toxicol. Pharmacol.* **2007**, *146*, 168−174.
(4) Lancisi, G. M. *De Noxiis Paludum Effluvius Eorumque Remediis.* Salvioni, J. M.: Rome, 1717.
(5) Kumar, S.; Guha, M.; Choubey, V.; Maity, P.; Bandyopadhyay, U. *Life Sci.* **2007**, *80*, 813−828.
(6) Combrinck, J. M.; Mabotha, T. E.; Ncokazi, K. K.; Ambele, M. A.; Taylor, D.; Smith, P. J.; Hoppe, H. C.; Egan, T. J. *ACS Chem. Biol.* **2013**, *8*, 133−137.
(7) Kaschula, C. H.; Egan, T. J.; Hunter, R.; Basilico, N.; Parapini, S.; Taramelli, D.; Pasini, E.; Monti, D. *J. Med. Chem.* **2002**, *45*, 3531−3539.
(8) Fong, K. Y.; Wright, D. W. *Future Med. Chem.* **2013**, *5*, 1437−1450.
(9) Egan, T. J.; Mavuso, W. W.; Ncokazi, K. K. *Biochemistry* **2001**, *40*, 204−213.
(10) Bohle, D. S.; Helms, J. B. *Biochem. Biophys. Res. Commun.* **1993**, *193*, 504−508.
(11) Huy, N. T.; Maeda, A.; Uyen, D. T.; Trang, D. T. X.; Sasai, M.; Shiono, T.; Oida, T.; Harada, S.; Kamei, K. *Acta Trop.* **2007**, *101*, 130−138.
(12) Sandlin, R. D.; Fong, K. Y.; Wicht, K. J.; Carrell, H. M.; Egan, T. J.; Wright, D. W. *Int. J. Parasitol.: Drugs Drug Resist.* **2014**, *4*, 316−325.
(13) Rush, M. A.; Baniecki, M. L.; Mazitschek, R.; Cortese, J. F.; Wiegand, R.; Clardy, J.; Wirth, D. F. *Antimicrob. Agents Chemother.* **2009**, *53*, 2564−2568.
(14) Ncokazi, K. K.; Egan, T. J. *Anal. Biochem.* **2005**, *338*, 306−319.
(15) Ambele, M. A.; Egan, T. J. *Malar. J.* **2012**, *11*, 1−13.33710.1186/1475-2875-11-337
(16) Jackson, K. E.; Klonis, N.; Ferguson, D. J. P.; Adisa, A.; Dogovski, C.; Tilley, L. *Mol. Microbiol.* **2004**, *54*, 109−122.
(17) Pisciotta, J.; Coppens, I.; Tripathi, A.; Scholl, P.; Shuman, J.; Bajad, S.; Shulaev, V.; Sullivan, D. *Biochem. J.* **2007**, *402*, 197−204.
(18) Hoang, A. N.; Sandlin, R. D.; Omar, A.; Egan, T. J.; Wright, D. W. *Biochemistry* **2010**, *49*, 10107−10116.
(19) de Villiers, K. A.; Kaschula, C. H.; Egan, T. J.; Marques, H. M. *JBIC, J. Biol. Inorg. Chem.* **2007**, *12*, 101−117.
(20) Kapishnikov, S.; Weiner, A.; Shimoni, E.; Guttmann, P.; Schneider, G.; Dahan-Pasternak, N.; Dzikowski, R.; Leiserowitz, L.; Elbaum, M. *Proc. Natl. Acad. Sci. U. S. A.* **2012**, *109*, 11188−11193.
(21) Kapishnikov, S.; Weiner, A.; Shimoni, E.; Schneider, G.; Elbaum, M.; Leiserowitz, L. *Langmuir* **2013**, *29*, 14595−14602.
(22) Kapishnikov, S.; Berthing, T.; Hviid, L.; Dierolf, M.; Menzel, A.; Pfeiffer, F.; Als-Nielsen, J.; Leiserowitz, L. *Proc. Natl. Acad. Sci. U. S. A.* **2012**, *109*, 11184−11187.
(23) Carter, M. D.; Phelan, V. V.; Sandlin, R. D.; Bachmann, B. O.; Wright, D. W. *Comb. Chem. High Throughput Screening* **2010**, *13*, 285−292.
(24) Stiebler, R.; Hoang, A. N.; Egan, T. J.; Wright, D. W.; Oliveira, M. F. *PLoS One* **2010**, *5*.e1269410.1371/journal.pone.0012694
(25) Stiebler, R.; Majerowicz, D.; Knudsen, J.; Gondim, K. C.; Wright, D. W.; Egan, T. J.; Oliveira, M. F. *PLoS One* **2014**, *9*.e8897610.1371/journal.pone.0088976
(26) Huy, N. T.; Shima, Y.; Maeda, A.; Men, T. T.; Hirayama, K.; Hirase, A.; Miyazawa, A.; Kamei, K. *PLoS One* **2013**, *8*.e7002510.1371/journal.pone.0070025
(27) Ncokazi, K. K.; Egan, T. J. *Anal. Biochem.* **2005**, *338*, 306−19.
(28) Provera, S.; Beato, S.; Cimarosti, Z.; Turco, L.; Casazza, A.; Caivano, G.; Marchioro, C. *J. Pharm. Biomed. Anal.* **2011**, *54*, 48−52.
(29) Huy, N. T.; Uyen, D. T.; Maeda, A.; Trang, D. T. X.; Oida, T.; Harada, S.; Kamei, K. *Antimicrob. Agents Chemother.* **2007**, *51*, 350−353.
(30) Pagola, S.; Stephens, P. W.; Bohle, D. S.; Kosar, A. D.; Madsen, S. K. *Nature* **2000**, *404*, 307−310.
(31) Wang, X.; Ingall, E.; Lai, B.; Stack, A. G. *Cryst. Growth Des.* **2010**, *10*, 798−805.
(32) Bohle, D. S.; Dinnebier, R. E.; Madsen, S. K.; Stephens, P. W. *J. Biol. Chem.* **1997**, *272*, 713−716.
(33) Slater, A. F. G.; Swiggard, W. J.; Orton, B. R.; Flitter, W. D.; Goldberg, D. E.; Cerami, A.; Henderson, G. B. *Proc. Natl. Acad. Sci. U. S. A.* **1991**, *88*, 325−329.
(34) Ambele, M. A.; Sewell, B. T.; Cummings, F. R.; Smith, P. J.; Egan, T. J. *Cryst. Growth Des.* **2013**, *13*, 4442−4452.
(35) Yonekura, R.; Grinstaff, M. W. *Phys. Chem. Chem. Phys.* **2014**, *16*, 20608−20617.
(36) Klonis, N.; Dilanian, R.; Hanssen, E.; Darmanin, C.; Streltsov, V.; Deed, S.; Quiney, H.; Tilley, L. *Biochemistry* **2010**, *49*, 6804−6811.
(37) Hoang, A. N.; Ncokazi, K. K.; de Villiers, K. A.; Wright, D. W.; Egan, T. J. *Dalton Trans.* **2010**, *39*, 1235−1244.
(38) Egan, T. J.; Chen, J. Y. J.; de Villiers, K. A.; Mabotha, T. E.; Naidoo, K. J.; Ncokazi, K. K.; Langford, S. J.; McNaughton, D.; Pandiancherri, S.; Wood, B. R. *FEBS Lett.* **2006**, *580*, 5105−5110.
(39) Falk, J. E. *Porphyrins and Metalloporphyrins: Their General, Physical and Coordination Chemistry, and Laboratory Methods*; Elsevier Pub. Co.: Amsterdam, 1964.
(40) Kumbhakar, M.; Nath, S.; Mukherjee, T.; Pal, H. *J. Chem. Phys.* **2004**, *121*, 6026−6033.

DOI: 10.1021/acs.cgd.5b01580
Cryst. Growth Des. 2016, 16, 2542−2551

(41) Avrami, M. *J. Chem. Phys.* **1939**, *7*, 1103.
(42) Egan, T. J.; Mavuso, W. W.; Ncokazi, K. K. *Biochemistry* **2001**, *40*, 204−213.
(43) Egan, T. J.; Tshivhase, M. G. *Dalton Trans.* **2006**, 5024−5032.
(44) Olafson, K. N.; Ketchum, M. A.; Rimer, J. D.; Vekilov, P. G. *Proc. Natl. Acad. Sci. U. S. A.* **2015**, *112*, 4946−4951.

DOI: 10.1021/acs.cgd.5b01580
Cryst. Growth Des. 2016, 16, 2542−2551